SOA-REAM Assisted Synaptic Receptor for Weighted-Sum Detection of Multiple Inputs

Margareta Vania Stephanie, *Student Member, IEEE*, Florian Honz, *Student Member, IEEE*, Nemanja Vokić, *Member, IEEE*, Winfried Boxleitner, Michael Waltl, *Senior Member, IEEE*, Tibor Grasser, *Fellow, IEEE* and Bernhard Schrenk, *Member, IEEE*

***Abstract*—Neuromorphic photonics is a promising research field due to its potential to tackle the limitations arising from the bottleneck of the von-Neumann computation architecture. Inspired by the characteristics and behavior of the biological brain, photonic neural networks are touted as a solution for solving complex problems that require GHz operation at low latency and low power consumption. An essential building block of such a neural network is a low-complexity multiply-accumulate operation, for which efficient functional implementations in the optical domain are sought for. Towards this direction, we present a synaptic receptor that functionally integrates weighting and signal detection. This optical multiply-accumulate operation is accomplished through a monolithic integrated semiconductor optical amplifier and reflective electro-absorption modulator, which together serve as a colorless frequency demodulator and detector of frequency-coded signals. Moreover, we show that two spike trains can be simultaneously processed with alternating signs and detected as a weighted sum. The performance of the proposed synaptic receptors is further validated through a low bit error ratio for signal rates of up to 10 Gb/s.**

***Index Terms*—Optical signal detection, Neural network hardware, Neuromorphic photonics, Synaptic receptor**

I. Introduction

Since the birth of the Information Age about half a century ago, the growth of data processing and generation is accelerating exponentially while current digital electronic computing architectures are hitting the brick-wall for further hardware scaling [1-3]. The longing for a new evolutionary step in the computing ecosystem has triggered scientists to learn and adopt how the human brain processes information. The human brain is considered as a natural biological computer that is able to learn, analyze and decide. It does so with short time delay and high energy efficiency, when compared to a digital computer [4]. Over the past few decades, the artificial neural network (ANN) has emerged as a powerful model to simulate the functional brain network [5]. With the demonstration of a successful coding algorithm for solving complex problems, tremendous efforts have focused on the development of intelligent machines based on ANNs [6-9].

Underpinned by currently available and rapidly maturing circuit integration technologies, photonics can bridge the gap between the human neuronal system and the conventional computer architecture. Marrying a bio-inspired ANN and photonic broadband technology gives birth to an emerging field so-called neuromorphic photonics. By utilizing the high speed, large bandwidth and massive parallelism of photonic devices, an optical neural network offers the possibility to break the limitation of conventional microelectronics, thus enabling low-latency multiply-accumulate (MAC) operations in a complex system that is destined for fast signal processing at GHz information rates [10].

Accomplishing efficient processing by optical means requires a set of operations equivalent to those of a neural network. This includes an architecture with a synaptic interconnect between neurons, which performs weighted summation and non-linear thresholding [11]. Earlier demonstrations in the field of neuromorphic photonics have focused on the linear MAC operation in a neural network, such as shown for a reconfigurable circuit based on a Mach-Zehnder interferometer (MZI) mesh [12, 13]. Although such a circuit is considered to be flexible when it comes to an expansion of its size, it is conceived for operation at a single wavelength, for which the phase control is limited to rather small kHz to MHz rates. Another approach is a fast coherent detection employing free-space optics that permit the scaling to a large number of neurons [14]. However, such an ANN implementation experiences scaling problems arising from phase instability and aberration, which motivate subsequent works to focus on integrated systems. One of such photonic integrated networks has been realized by dedicating different wavelengths to different input signals while using the wavelength-specific transfer function of micro-ring resonators to yield a compact weight bank [15]. Apart from its compatibility with wavelength division multiplexing (WDM), the summation of positive and negative weights necessitates the use of both, drop and pass-through ports of the resonator,

Manuscript received May 31, 2022. This work was supported by the European Research Council (ERC) under the European Union's Horizon 2020 programme (grant agreement No 804769) and by the Austrian FFG agency through the JOLLYBEE project (grant No. 887467).

M. V. Stephanie, F. Honz, N. Vokić, W. Boxleitner, and B. Schrenk are with the AIT Austrian Institute of Technology, Center for Digital Safety&Security, Giefinggasse 4, 1210 Vienna, Austria (e-mail: margareta.stephanie@ait.ac.at).

M. Waltl and T. Grasser are with the Institute for Microelectronics, TU Wien, Gusshausstrasse 27-29, 1040 Vienna, Austria (e-mail: waltl@iue.tuwien.ac.at; grasser@iue.tuwien.ac.at).

This article has been accepted for publication in IEEE/OSA Journal of Lightwave Technology. This is the author's version which has not been fully edited and content may change prior to final publication. Citation information: DOI 10.1109/JLT.2022.3212111

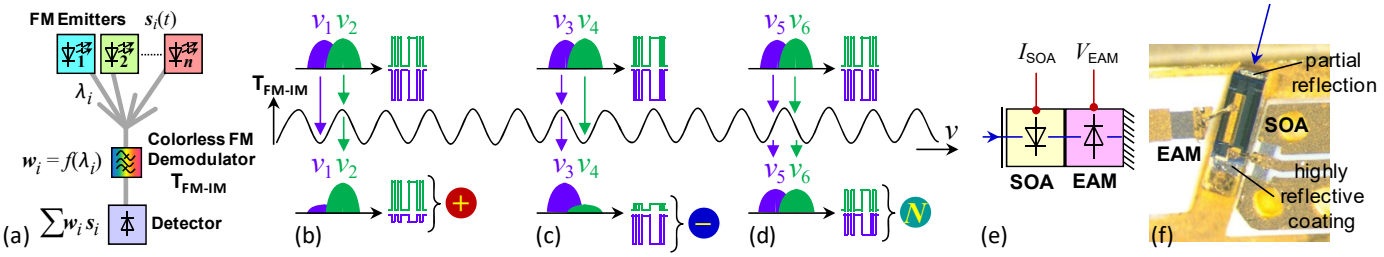

Fig. 1. (a) Architectural overview of the synaptic interconnect and principal operation of weight tuning with (b) positive and (c) negative sign, including also the possibility to set the magnitude of the weight, as sketched for the extreme case (d) of having zero magnitude. (e) Proposed synaptic receptor based on SOA-REAM and (f) device employed in the experiment.

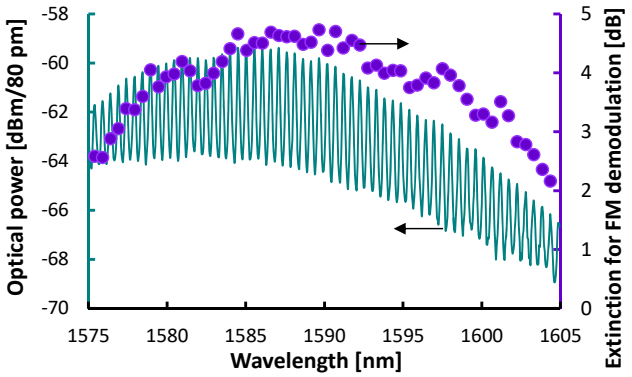

Fig. 2. Comb-like SOA-REAM emission spectrum indicating a periodic FM-to-IM conversion function and corresponding extinction characteristics.

in combination with a balanced photodetector. Alternative methods have been proposed on more specific integration platforms, such as shown for phase-change materials on optical waveguides. In this scheme the synaptic weight can be controlled by changing the number of optical pulses sent through the waveguide [16, 17]. However, the use of an auxiliary external probe laser is not desired for a highly integrated ANN application.

In this work, we demonstrate an integrated synaptic receptor for the weighting of frequency-coded signals with information rates up to 10 Gb/s. A semiconductor optical amplifier (SOA) is used to form an active detector cavity that performs a sign- and magnitude-tunable frequency-to-intensity conversion for the received signals, which are then detected by a reflective electro-absorption modulator (REAM). We further show that the spectrally periodic and comb-like demodulation function of the cavity is compatible with the simultaneous processing of multiple synapses at different wavelengths. Therefore, the monolithically integrated SOA-REAM receptor is able to perform wideband demodulation and detection, as experimentally demonstrated for a linear MAC operation performing weighing and summation of two spike trains with a spectral detuning of 23 nm. We extend our initial study [18] by further proving the successful integration of detection functionality within the synaptic receptor cavity.

The paper is organized as follows. Section II covers the fundamental idea of frequency-coded synapses in view of integrating weighting functionality with a SOA-REAM as a synaptic receptor. Section III discusses the experimental setup, while Section IV presents a characterization of the synaptic receptor and elaborates on its reception performance. Section V reports on the integration of photodetection functionality with the synaptic receptor. Finally, Section VI summarizes the work and concludes with an outlook for further improvement.

II. Synaptic Receptor for Frequency Coded Signals

A. Setting Sign and Magnitude for Weighted Detection

The linear operation of MAC is basically at the heart of optical neurons, where signals traversing a synaptic interconnect are weighted and linearly summed. In this work we propose a frequency-coded signal representation in this interconnect, which is introduced in Fig. 1(a). We accomplish weight assignment during the frequency-to-intensity demodulation process, as exemplarily highlighted in Fig. 1(b-d). This translation of a frequency modulated (FM) signal to an intensity modulated (IM) signal before frequency-agnostic photodetection requires a comb-like transfer function $T_{\text{FM-IM}}$, whose periodicity can be exploited for a simultaneous weighting of multiple input signals. In this regard, we use an amplified cavity comprising of a SOA with pronounced gain ripple, further comprising of a REAM for integrated weighted photodetection (Fig. 1(e)). The wavelength-selective gain spectrum can be expressed through the transfer function T_{rx} for signal detection according to [19]

$$T_{rx} = \frac{1}{1-R} \frac{(1-R)^2 G_{soa} a_{eam}}{(1+R G_{soa} a_{eam})^2 + 4R G_{soa} a_{eam} \sin^2\left(\frac{2\pi \nu_{in}}{FSR}\right)} \quad (1)$$

where R is the residual front facet reflectivity, G_{soa} and a_{eam} are the SOA gain and the EAM loss, ν_{in} is the optical frequency of the input signal and FSR is the free spectral range of the SOA-REAM cavity.

The artificial ripple in the spectral response will serve the demodulation of the frequency-coded synapses. In Fig. 1(a), the FM demodulator as part of the synaptic receptor leads to a weight setting w_i for a given wavelength channel λ_i. This setting depends on the spectral alignment of λ_i relative to the comb-like transfer function $T_{\text{FM-IM}} = T_{rx}$. The alignment is governed by tuning either the comb or the wavelength of the input signal s_i. Since the SOA gain ripple supports operation over a wide optical bandwidth, allowing us to facilitate multiple wavelength channels, the weighted addition of all present emitters will be received by the photodetector, by virtue of the wide optical bandwidth of the photodiode. Therefore, the SOA-REAM cavity can be used as a colorless demodulator, whereas the term “colorless” does not refer to a wavelength-agnostic behavior but instead relates to the fact that multiple channels can be spectrally processed with the

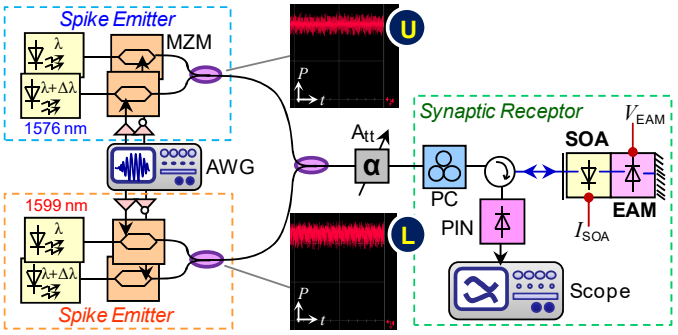

Fig. 3. Experimental setup to evaluate the reception performance of the synaptic receptor and to perform simultaneous weighing and summation of the signals from two different spike emitters.

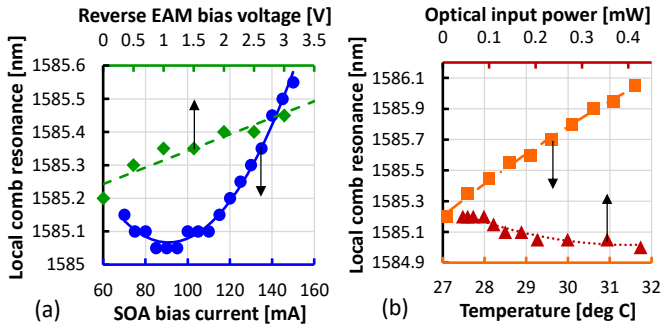

Fig. 4. Spectral detuning of the SOA-REAM transfer function related to (a) SOA and EAM biases, and (b) temperature and optical input power.

same transfer function T_{rx}, owing to its periodic transmission property.

The spectral alignment of the FM signal to the comb transfer function is illustrated in Fig. 1(b-d) for various weight settings. Depending on the spectral allocation of the mark (ν_2, ν_4, ν_6) and space (ν_1, ν_3, ν_5) bit of the FM signal, the resulting IM signal can be assigned to a positive (+) or negative (–) weight. This is accomplished through selecting the corresponding FM tributary, such as ν_2 in case of a positive weight. The magnitude of the weight is tuned through the relative alignment of the FM tributaries with respect to the comb function $T_{FM\text{-}IM}$. A high extinction and thus the largest magnitude is obtained by maximally suppressing one of the tributaries while passing the other, as sketched in Fig. 1(b) for the positive (ν_2 passes, ν_1 suppressed) and in Fig. 1(c) negative (ν_3 passes, ν_4 suppressed) cases. For the sake of completeness, it shall be stressed that a zero magnitude for the weight occurs when both tributaries experience the same transmission during FM-to-IM conversion, as shown for ν_5 and ν_6 in the setting denoted as *N* in Fig. 1(d).

Practically, the sign and magnitude of the weight can be set through detuning the comb function via several parameters that cause a change of the optical density within the SOA-REAM cavity, as will be characterized shortly. The extreme case of inverting the sign while retaining maximal magnitude can be accomplished straightforwardly by shifting the transfer function by half of its FSR.

In a synaptic interconnect with many emitters and a single synaptic receptor, a spectral alignment at the emitter side might be more convenient. This alternative approach is backed by the availability of low-complexity tunable lasers [20-22].

B. Synaptic Emitter and Receptor

The synaptic emitter is required to encode its signals in optical frequency. Since a modulation of laser current generally leads to a variation in optical frequency [23], the adiabatic chirp property of a directly modulated laser (DML), which describes a linear optical power dependence of the refractive index, can be exploited to generate the FM signals traversing the synaptic interconnect. These FM signals have their mark bits blue-shifted relative to their space bits, yielding the FM-specific signal spectrum with the two aforementioned tributaries (ν_2 and ν_1). For the specific application in an ANN, this frequency coding can be translated as a signal representation where the mark bit represents an active synapse (i.e., a spike is emitted) at frequency ν_2, while the space bit corresponds to an inactive synapse at ν_1 (i.e., emitter at rest with no spike being emitted). These two spectral components of the FM signal play an important role in setting the sign of the detected signal, which is done by suppressing the tributaries through the periodic transfer function of the detector, as shown in Fig. 1(b-d).

The synaptic receptor, which is the main scope of this work, is shown in Fig. 1(f). The front facet of SOA is partially reflective, while the end facet of REAM is highly reflective. Consequently, the feedback at both facets of the SOA-REAM cavity part leads to the formation of a gain ripple with Fabry-Perot characteristics as intended for the purpose of FM-to-IM conversion. The SOA-REAM had a length of ~470 µm, which results in a FSR of 0.55 nm. The corresponding transfer function for the used L-band SOA-REAM is reported in Fig. 2. It shows a moderate contrast between maximum and minimum transmission points, leading to a peak extinction of 4.73 dB (Fig. 2; ●). The gain spectrum of the SOA has a 3-dB optical bandwidth of 23.75 nm. Therefore, the optical comb function of the SOA-REAM can support 43 synapses, considering that the spacing is determined by the FSR of 0.55 nm. The EAM itself plays an important role in optical communications not only for transmitting, but also for receiving optical signals [24]. Its operation is based on the Franz-Keldysh effect, yielding an absorption spectrum that can be efficiently shifted by applying an electric field. A rather low driving voltage can induce a high intensity extinction ratio for optical modulation or support broadband photodetection. Towards the latter, the co-integrated SOA serves as an optical pre-amplifier for the EAM photodiode. Thus, the monolithic integration of SOA and REAM can serve as a colorless demodulator and detector.

III. Experimental Setup

Figure 3 shows the experimental setup to evaluate the reception of frequency-coded synapses with the proposed FM-to-IM converter. Two upstream spike emitters at 1576 and 1599 nm are connected to the downstream synaptic receptor. Since no L-band DML was available, each emitter consisted of a pair of Mach-Zehnder modulators (MZM) to generate an FM signal through complementary intensity modulation of the

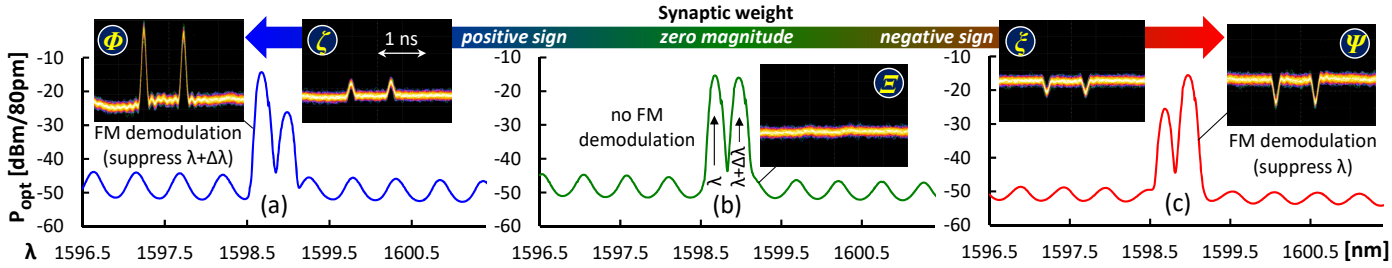

Fig. 5. Spectra of signal and spike train reception of SOA-REAM with different weighing processes (a) positive sign, (b) zero magnitude, and (c) negative sign.

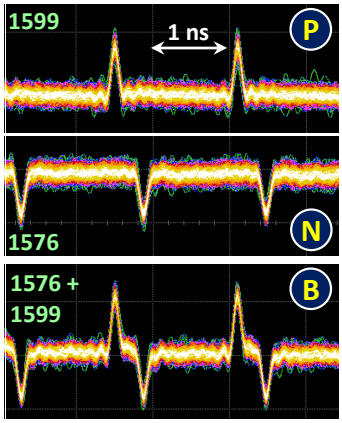

Fig. 6. Simultaneous reception of weighted spike trains summed by the synaptic receptor (B) where the constituent wavelength channels at 1576 and 1599 nm are weighted negatively (N) and positively (P), respectively.

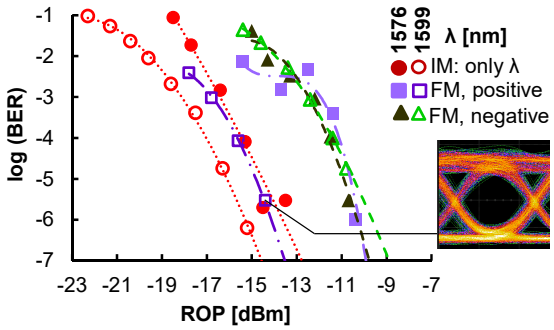

Fig. 7. BER performance of the SOA-REAM serving as a colorless demodulator for frequency-coded synapses.

FM tributaries at λ and λ+Δλ, respectively – corresponding to v_2 and v_1 in Fig. 1(b-d). The complementary outputs are combined with a 50/50 splitter and the difference Δλ between the two optical sources for the same wavelength channel is fine-tuned to the comb function so that Δλ = FSR/2. An arbitrary waveform generator (AWG) is used to drive the modulators with two sets of waveforms. The first is a spike train with 100-ps spike width and a duty cycle of 1/16. The timing parameters of this spike train is conceived to leave enough room for time-interleaving of a second spike train that is spectrally allocated along the comb function. The second waveform is a 10 Gb/s pseudo-random bit sequence for bit error ratio (BER) measurements. The resulting intensity extinction ratio for the generated FM signals is 0.72 dB and their constant-power output is -1 dBm (**U** and **L** in Fig. 3).

The synaptic receptor includes the SOA-REAM and a polarisation controller (PC) to compensate for the polarisation-dependent response of the EAM. In this first experiment, a PIN receiver is added as an external photodetector. Finally, the demodulated synapses are digitized through a real-time scope. For the purpose of BER measurements, we included a variable optical attenuator (A_{tt}) to change the received optical power (ROP) at the downstream receptor.

IV. Results and Discussion

A. Weight tuning and simultaneous summation of signals

The weight of the proposed receptor is determined in both, sign and magnitude, by the relative spectral alignment of the input signal to the comb transfer function of the SOA-REAM. The characterization of the spectral tuning of the comb function is reported in Fig. 4 for several parameters that induce a variation in the optical density of the SOA-REAM cavity. This includes SOA and EAM biases (Fig. 4(a)), temperature and input signal power (Fig. 4(b)). The characterization results are shown as the spectral detuning of a local comb resonance around 1585 nm, which is in the middle of the gain spectrum. In the case of varying SOA bias current, the local resonance is blue-shifted until the threshold of ~95 mA is reached. To accomplish a sufficiently high cavity gain is then linearly red-shifted at a response of 1.34 GHz/mA (● in Fig. 4(a)). For the EAM bias we see a linear dependence on the bias voltage at a detuning of 9.94 GHz/V (◆ in Fig. 4(a)). The detuning further shows a rather large temperature sensitivity with a response of 22.5 GHz/°C (■ in Fig. 4(b)). We found the optical input power affecting the resonance by a spectral shift of -155.6 GHz/mW (▲ in Fig. 4(b)) in the range between -13.6 dBm (~0 mW) and -3.7 dBm (~0.4 mW). Given the small variation in delivered optical power for synaptic interconnects with defined optical budget, this detuning could be compensated through initial receptor calibration.

Figure 5 shows the optical signal spectra for the demodulated FM signal at 1599 nm at the output of the SOA-REAM after FM-to-IM conversion. The spectra are presented for various weight settings and their corresponding detuning of the comb function. Since there are two emitters and one synaptic receptor, it was required to perform an independent spectral alignment for at least one of the two spike emitters by tuning the temperature or current of its distributed feedback (DFB) laser source. In addition, the insets in Fig. 5 show the received spike trains for each weight setting. By suppressing the optical FM tributary at λ+Δλ or at λ, a positive (*Φ*) or a negative (*Ψ*) sign can be accomplished for the detected spike train, respectively. When there is no FM demodulation

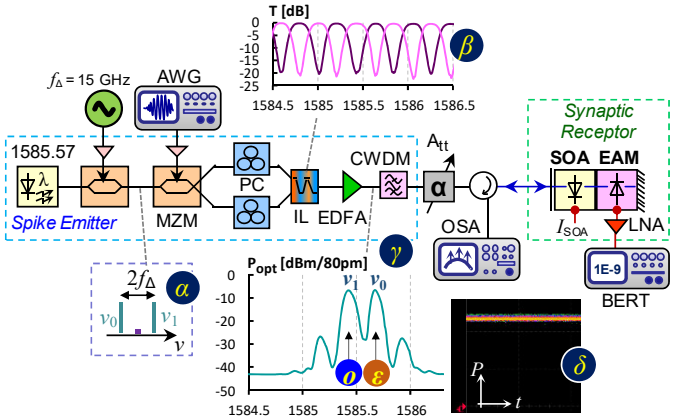

Fig. 8. Experimental setup for evaluating the SOA-REAM as a colorless demodulator and detector for frequency-coded synapses.

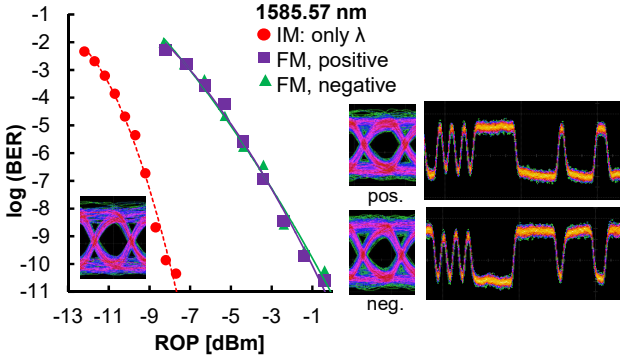

Fig. 9. BER performance of the SOA-REAM serving as colorless demodulator and detector of frequency-coded synapses.

imposed, the received signal has a constant amplitude (Ξ), equivalent to a zero magnitude of the weight. By detuning the comb, the magnitude of the weight can be varied, which is shown for the detected spike trains with reduced amplitude for a positive (ζ) and a negative sign (ξ).

In addition, two synaptic emitters have been jointly delivered to the SOA-REAM (Fig. 6). In this scenario, the 1599-nm signal has been chosen to be weighted positively (P), while the signal at 1576 nm is chosen with a negative sign (N). When applying both constituent signals at the input of the SOA-REAM at the same time, the received spike train yields a correctly summed output (B), as evidenced in Fig. 6. This result emphasizes the potential of the proposed synaptic receptor to perform larger MAC operations involving multiple synapses through exploiting the WDM dimension and the colorless behavior of the SOA-REAM.

B. Reception performance

The reception performance of the demodulated FM signals was evaluated in terms of BER measurements. Figure 7 shows the BER for the two wavelength channels as a function of the ROP at SOA-REAM. For each of the two channels, results are presented for a positive (suppressed λ+Δλ) and a negative (suppressed λ) weight. Comparison is further made with the reception of an IM signal, meaning that only the FM tributary at λ is modulated at the spike emitter. This case of receiving an IM signal is equivalent to the ideal case of an infinite extinction ratio for FM-to-IM conversion.

In general, a low BER can be obtained, despite the finite contrast in the SOA-REAM comb function and the moderate extinction for FM demodulation, as mentioned in Section III. For the first channel at 1576 nm (Fig. 7) we obtained a reception sensitivity of -10.4 dBm at a BER of 10^{-6} after FM demodulation (■, ▲), with a negligible difference of 0.1 dB between the positive and negative weight settings (■, ▲). There is a penalty of 3.2 dB with respect to the IM signal (●), which benefits from the high intensity extinction ratio of the MZM transmitter as it does not require FM demodulation. For the second channel at 1599 nm (Fig. 7) the sensitivities are -14.1 and -9.6 dBm for the positive (□) and the negative (△) weight, respectively, whereas the IM input features a reception sensitivity of -15.3 dBm (○). The improved sensitivity for the IM signals with respect to the reception of the FM signals is attributed to the reduced intensity extinction ratio after FM-to-IM conversion, as it results from the moderate contrast in the SOA-REAM comb function.

V. Synaptic Receptor with Integrated Detector

The capability of the SOA-REAM to integrate photodetection functionality was evaluated in a second experimental study, for which the setup is presented in Fig. 8. The generation of the FM signal at λ = 1585.57 nm is conducted through the generation of two optical carriers with the first MZM biased for carrier-suppressed double-sideband (CS-DSB) modulation. The two resulting spectral lines at ν_0 and ν_1 are then spaced by $2f_\Delta$ = 30 GHz (*α*). A second 1×2 MZM with complementary output ports modulates both lines with the same pseudo-random bit sequence at a data rate of 2.5 Gb/s. We connected both outputs to an optical 25/50 GHz interleaver (IL), which passed only one of the IM lines from each MZM output branch. This line selection is accomplished through the good suppression of 20.4 and 19.6 dB between neighbouring odd and even channels (*β*), which ensures a low crosstalk between the FM tributaries at ν_0 and ν_1. Therefore, we obtain a constant-power FM signal with only the tributary at ν_1 (***o***) and ν_0 (***e***) being found in the lower and upper sideband of the suppressed optical carrier λ, respectively (γ). The spectrum of the FM signal further indicates a good optical carrier suppression of 16.8 dB after CS-DSB modulation. It is important to note that the spectral configuration of the FM signal, in particular $|\nu_1 - \nu_0|$, is not only adjusted in view of the FSR/2 parameter of the demodulating comb function, but also in trade-off with a good suppression through the even / odd transmission windows of the IL. Due to this, the spacing $|\nu_1 - \nu_0| = 2f_\Delta$ is slightly less than FSR/2. It is worth to note that the specific FM emitter implementation of this second experimental study was primarily chosen for a more simplified handling of the FM configuration and is not a prerequisite for the proposed synaptic receptor.

The residual IM patterning of the transmitted FM signal had an extinction ratio of 0.26 dB (*δ*) and the state-of-polarisation at each of the single-mode fiber ports of the IL was aligned with a PC to ensure co-polarized FM tributaries at its output. The signal is boosted with an L-band Erbium-doped fiber

amplifier (EDFA) and the amplified spontaneous emission (ASE) peak is filtered with a 1591-nm coarse-WDM (CWDM) filter.

In this second synaptic receptor configuration, the EAM now serves as a photodiode. The detected photocurrent of the EAM is post-amplified with a 50Ω low-noise amplifier (LNA) due to the incompatible EAM interface for co-integration with a transimpedance amplifier (TIA). The reception performance has been evaluated through real-time BER measurements as a function of the ROP.

The FM demodulation of this second synaptic receptor featured a slightly higher extinction of 4.9 dB, compared to the synaptic receptor in the first experiment (Section II). The BER performance, shown in Fig. 9, proves that a low BER of 10^{-10} can be achieved. The corresponding reception sensitivities are -8 and -0.9 dBm for an IM input (●) and the FM demodulated signals, respectively. The rather high ROP is explained by the sub-optimal EAM-LNA receiver configuration, followed by the mode mismatch between the tapered single-mode fiber and the asymmetric cross-section of the InP waveguide of the SOA-REAM. The penalties inherent to the reception of the demodulated FM signals are 7 and 7.2 dB for a positive (■) and a negative (▲) weight, respectively. They are attributed as follows: 3 dB are dedicated to the suppression of optical power residing in one of the tributaries (either v_0 or v_1) in case of FM-to-IM conversion, which do not apply for the IM signal. In addition, a penalty in sensitivity of 2.9 dB applies due to a reduced extinction ratio of the demodulated IM signal [25]. However, Fig. 9 evidences that there is no BER floor and the eye diagrams are clearly open for both, the positively and the negatively weighted input signal.

VI. Conclusion

Neuromorphic photonics is a compelling field, able to untangle the limitations of current electronic computing architectures – provided that low-complexity solutions can be found. Towards this direction, we have experimentally demonstrated the flexibility that resides in frequency coding at the synaptic interconnect. We have shown that the monolithic integration of SOA and REAM can be used as a colorless synaptic receptor that permits the adjustment of sign and magnitude to perform linear MAC operations with a simplified receiver. WDM operation has been proven through the joint demodulation and detection of two spike trains with a spectral detuning of 23 nm, thus enabling a highly parallel synaptic interconnect. Moreover, the integration of detection functionality with the weight-tunable FM demodulator has been experimentally demonstrated and confirmed through a low BER. Our work leaves room for further improvement: A co-integration of an EAM photodiode and a noise-optimized TIA can boost the sensitivity of the receptor, while the seamless co-integration with a non-linear activation function for a functionally complete optical neuron is left for future work.

References

[1] P. J. Winzer and D. T. Neilson, "From scaling disparities to integrated parallelism: A decathlon for a decade," *J. Lightwave Technol.* vol. 35, no. 5, pp. 1099-1115, Mar. 2017.

[2] N. Jones, "The Information Factories," *Nature*, vol. 561, pp. 163-166, Sep. 2018.

[3] J. D. Kendall, and S. Kumar, "The building blocks of a brain-inspired computer," *Appl. Phys. Rev.* vol. 7, no. 1, Mar. 2020, Art. no. 011305,

[4] J. Hasler and B. Marr, "Finding a roadmap to achieve large neuromorphic hardware systems," *Front. Neurosci.*, vol. 7, no. 118, pp. 1-29, Sep. 2013.

[5] Y. LeCun, Y. Bengio and G. Hinton, "Deep learning," *Nature* vol. 521, pp. 436-444, May 2015.

[6] S. Furber, F. Galluppi, S. Temple, and L. Plana, "The SpiNNaker project," *Proc. IEEE*, vol. 102, pp. 652-665, May 2014.

[7] J. Shen et al., "Darwin: A neuromorphic hardware co-processor based on spiking neural networks," *Sci. China Inf. Sci.*, vol. 59, no. 2, pp. 1-5, Feb. 2016.

[8] M. Davies et al., "Loihi: A neuromorphic manycore processor with on-chip learning", *IEEE Micro*, vol. 38, no. 1, pp. 82-99, Jan. 2018.

[9] M. DeBole et al., "TrueNorth: Accelerating From Zero to 64 Million Neurons in 10 Years", *Computer J.*, vol. 52, no. 5, pp. 20-29, May 2019.

[10] P. R. Prucnal and B. J. Shastri, *Neuromorphic Photonics*. Boca Raton, FL, USA: CRC Press, May 2017.

[11] H. T. Peng, M. A. Nahmias, T. Ferreira de Lima, A. N. Tait, B. J. Shastri and P. R. Prucnal, "Neuromorphic photonic integrated circuits," *IEEE J. Sel. Topics Quantum Electron.*, vol. 24, no. 6, pp. 1–15, Nov. 2018.

[12] F. Shokraneh, S. Geoffroy-Gagnon, M. S. Nezami and O. Liboiron-Ladouceur, "A single layer neural network implemented by a 4 × 4 MZI-based optical processor," *IEEE Photonics. J.*, vol. 11, no. 6, pp. 1-12, Dec. 2019.

[13] Y. Shen, et al., "Deep learning with coherent nanophotonic circuits," *Nature Photon.*, vol. 11, pp. 441–446, Jun. 2017.

[14] R. Hamerly, L. Bernstein, A. Sludds, M. Soljačić, and D. Englund, "Large-Scale Optical Neural Networks Based on Photoelectric Multiplication," *Phys. Rev. X*, vol. 9, no. 2, May 2019, Art. no. 021032.

[15] A. Tait, M. A. Nahmias, B. J. Shastri, and P. R. Prucnal, "Broadcast and weight: An integrated network for scalable photonic spike processing," *J. Lightw. Technol.*, vol. 32, no. 21, pp. 3427-3439, Nov. 2014.

[16] Z. Cheng, C. Ríos, W. H. P. Pernice, C. D. Wright and H. Bhaskaran, "On-chip photonic synapse," *Sci. Adv.*, vol. 3, no. 9, Sep. 2017, Art. no. e1700160.

[17] M, Miscuglio et al., "Artificial Synapse with Mnemonic Functionality using GSST-based Photonic Integrated Memory," in *Proc. Int. Appl. Comput. Electromagn. Soc. Symp.*, IEEE, Jul. 2020, pp. 1-3.

[18] M. V. Stephanie, M. Waltl, T. Grasser and B, Schrenk, "WDM-Conscious Synaptic Receptor Assisted by SOA+EAM", in *Proc. Opt. Fib. Comm. Conf. (OFC)*, San Diego, United States, Mar. 2022, paper M1G.2.

[19] B. Schrenk, J.A. Lazaro, C. Kazmierski, and J. Prat, "Colorless FSK Demodulation and Detection With Integrated Fabry-Pérot Type SOA/REAM," *IEEE Phot. Technol. Lett.*, vol. 22, no. 13, pp. 1002-1004, Jul. 2010.

[20] L. Q. Yu *et al.*, "A widely tunable directly modulated DBR laser with high linearity," *IEEE Phot. J.*, vol. 6, no. 4, p. 1501308, Aug. 2014.

[21] T. Chu, N. Fujioka, and M. Ishizaka, "Compact, lower-power consumption wavelength tunable laser fabricated with silicon photonic wire waveguide micro-ring resonators," *Opt. Expr.*, vol. 17, no. 16, pp. 14063-14068, Aug. 2009.

[22] J.M. Fabrega *et al.*, "Modulated Grating Y-Structure Tunable Laser for λ-Routed Networks and Optical Access", *IEEE J. Sel. Topics in Quantum Electron.*, vol. 17, pp. 1542-1551, Nov. 2011.

[23] J. J. Martinez, J. I. G. Gregorio, A. L. Lucia, A. V. Velasco, J. C. Aguado, and M. A. L. Binue, "Novel WDM-PON architecture based on a spectrally efficient IM-FSK scheme using DMLs and RSOAs," *J. Lightw. Technol.*, vol. 26, no. 2, pp. 350–356, Feb. 2008.

[24] B. Schrenk, "The Electroabsorption-Modulated Laser as Optical Transmitter and Receiver: Status and Opportunities," *IET Optoel*., vol. 14, no. 6, pp. 374-385, 2020.

[25] B. Schrenk et al., "All-Optical Carrier Recovery Scheme for Access Networks with Simple ASK Modulation," *J. Opt. Comm. and Netw.*, vol. 3, pp. 704-712, Sept. 2011.

Margareta Vania Stephanie was born 1995 in Indonesia. She obtained B.Sc. ('17) degree in Physics from Bandung Institute of Technology, Indonesia, and M.Sc. ('21) degree in Photonics from Friedrich-Schiller-University of Jena, Germany. She is currently working toward the Ph.D. degree focused on photonic neural networks for hardware-accelerated artificial intelligence applications at AIT Austrian Institute of Technology and Technical University of Vienna.

Florian Honz was born in Austria, in 1994. He received his M.Sc. degree in Technical Physics in 2020 from the Technical University of Vienna. For his master thesis he joined the Quantum Metrology research group of Prof. Schumm at the Technical University of Vienna, where he contributed to the development of a Caesium interferometer utilizing the features of matter waves for metrology. Since 2021, he is with the AIT Austrian Institute of Technology, Vienna, working towards his Ph.D. degree in the field of photonics and quantum communications.

Nemanja Vokić was born in Serbia in 1990. He received the M.Sc. degree in electrical and computer engineering from the University of Novi Sad, Novi Sad, Serbia in 2014. He obtained his Ph.D. degree from Vienna University of Technology, Vienna, Austria in 2018. For his Ph.D. work, he designed full-custom electronic integrated circuits for transmitters and receivers for broadband optical communications. He was then a post-doc at Vienna University of Technology, designing mm-wave ASICs for 5G remote radio heads. In 2019, he joined AIT Austrian Institute of Technology, Vienna, Austria. His research interests include design of analog, RF, as well as photonic integrated circuits, opto-electronic circuit integration, coherent optical communication for telecom, datacom and quantum communications.

Winfried Boxleitner received his M.Sc in Physics at the University of Innsbruck in 1992. He received his Ph.D. from Vienna University of Technology, Austria under Prof. Erich Gornik in 1997 and worked on quantum transport in semiconductor heterostructures. He held a post-doctoral position at the Institute for Solid State Electronics at Vienna University of Technology from 1997 to 2003, when he joined the Opto-Electronic-Engineering group at AIT (Austrian Institute of Technology), Vienna. At AIT, his focus is on Computational Physics and design of Photonic Integrated Circuits.

Michael Waltl is an Assistant professor at TU Wien in Vienna, Austria. He received his Master's degree (Dipl.-Ing.) and his doctoral degree (Dr.techn.) in Microelectronics from TU Wien in 2011 and 2016, respectively. His overall scientific focus is on the robustness of microelectronic devices and circuits. In this field, he investigates reliability issues – characterization and modeling – in transistors and circuits made from 2D materials, Si, and wide bandgap materials such as SiC.

Tibor Grasser is an IEEE Fellow and head of the Institute for Microelectronics at TU Wien. He has edited various books, e.g. on the bias temperature instability, hot carrier degradation, and low-frequency noise (all with Springer), is a distinguished lecturer of the IEEE EDS, has been involved in outstanding conferences such as IEDM (General Chair 2021), IRPS, SISPAD, ESSDERC, and IIRW, is a recipient of the Best and Outstanding Paper Awards at IRPS (2008, 2010, 2012, and 2014), IPFA (2013 and 2014), ESREF (2008) and the IEEE EDS Paul Rappaport Award (2011). He currently serves as an Associate Editor for IEEE T-ED, following his assignment with Microelectronics Reliability (Elsevier).

Bernhard Schrenk (S'10-M'11) was born 1982 in Austria and received the M.Sc. ('07) degree in microelectronics from the Technical University of Vienna. He was at the Institute of Experimental Physics of Prof. A. Zeilinger, where he was involved in the realization of a first commercial prototype for a quantum cryptography system, within the European SECOQC project. From 2007 to early 2011 he obtained his Ph.D degree at UPC BarcelonaTech, Spain. His Ph.D thesis on multi-functional optical network units for next-generation Fiber-to-the-Home access networks was carried out within the FP7 SARDANA and EURO-FOS projects. In 2011 he joined the Photonic Communications Research Laboratory at NTUA, Athens, as post-doctoral researcher and established his research activities on coherent FTTH under the umbrella of the FP7 GALACTICO project. In 2013 he established his own research force on photonic communications at AIT Austrian Institute of Technology, Vienna, where he is working towards next-generation metro-access-5G networks, photonics integration technologies and quantum optics.
Dr. Schrenk has authored and co-authored ~190 publications in top-of-the-line (IEEE, OSA) journals and presentations in the most prestigious and highly competitive optical fiber technology conferences. He was further awarded with the Photonics21 Student Innovation Award and the Euro-Fos Student Research Award. He was elected as Board-of-Stakeholder member of the Photonics21 European Technology Platform in 2017 and is serving as Technical Program Committee member for the ECOC and OFC conferences. During his extensive research activities he was and is still engaged in several European projects such as SARDANA, BONE, BOOM, APACHE, GALACTICO, EURO-FOS and the Quantum Flagship project UNIQORN. In 2013 he received the European Marie-Curie Integration Grant WARP-5. In 2018 he was awarded by the European Research Council with the ERC Starting Grant COYOTE, which envisions coherent optics everywhere.